Libyan Open University Journal of Applied Sciences (LOUJAS)
Volume 2 - Issue 2 - 2026 - Pages 62-71

Optimization of TIG Welding Parameters for AISI 304 Stainless Steel Using Conventional and Hybrid Tungsten Electrodes: Mechanical Performance, Radiographic Evaluation, Hardness Distribution, and Numerical Simulation

AbdelSamad Mohammed Al-Falah *[1], Ahmed Salem Elmaalul[2], Esmail Ramadan El-sghayer[3], Mohamed Abdulghani Albashir Shamli[4], Emhemed Adel Zarouq[5]
[1,2] Department of Mechanical and Industrial Engineering, Faculty of Engineering, University of Tripoli, Libya
[3]Libyan Advanced Vocational Center for Welding Technologies, Tripoli, Libya
[4,5]Trainee at the Department of Mechanical Engineering, University of Tripoli, Libya
*Email for reference researcher: Ah.Elmaalul@uot.edu.ly

تحسين معاملات عملية لحام القوس التجستين والغاز الخامل (TIG) للفولاذ المقاوم للصدأ AISI 304 باستخدام أقطاب تنجستين تقليدية وهجينة: و دراسة الأداء الميكانيكي، والتقييم الإشعاعي، وتوزيع الصلادة، والمحاكاة العددية

عبد الصمد محمد الفلاح*[1]، أحمد سالم المعلول[2]، اسماعيل رمضان الصغير[3]، محمد عبد الغني الشاملي[4]، إمحمد عادل الزروق [5]
[1،2] قسم الهندسة الميكانيكية و الصناعية ، كلية الهندسة ، جامعة طرابلس ، ليبيا
[3] المركز الليبي المتقدم لتقنيات اللحام ، طرابلس ، ليبيا
[4،5]متدرب في قسم الهندسة الميكانيكية ، جامعة طرابلس، ليبيا

Received: 07-05-2026; Accepted: 06-07-2026; Published: 09-07-2026

Abstract
TIG welding is widely used for joining austenitic stainless steels because of the clean, controlled welds it produces with minimal contamination. In this work, we examined how nine different tungsten electrode types affect the weld quality of 3 mm AISI 304 stainless steel plates under direct-current conditions at three current settings: 60 A, 70 A, and 80 A, with argon shielding throughout.
Weld quality was evaluated through tensile and bend testing, radiographic examination, microhardness profiling, and finite-element simulation. The results show a clear performance advantage for hybrid electrodes over conventional ones. Among all tested configurations, the MX2 hybrid electrode at 70 A gave the highest tensile strength,around 772 Mpa-with elongation values above 100%. Radiographic inspection of these welds showed very few internal defects. Based on our findings, welding currents in the 60–70 A range appear best suited for this material and thickness.

Keywords: AISI 304 stainless steel, TIG welding, GTAW, tungsten electrode, hybrid electrode, tensile strength, radiographic testing, hardness, finite element analysis.

الملخص.
يُستخدم اللحام لتنجستين (TIG) على نطاق واسع لوصل الصلب الذي لا يصدأ ، نظراً لما ينتجه من وصلة لحام نظيفة ومُحكمة مع الحد الأدنى من العيوب ، تدرس هذه الورقة مدى تأثير أنواع مختلفة من أقطاب التنجستين على جودة اللحام لألواح من الصلب الذي لا يصدأ من النوع (AISI 304) و بسُمك 3 مم، عند ظروف التيار المستمر وباستخدام ثلاثة إعدادات للتيار: 60 أمبير، 70 أمبير، و 80 أمبير، مع استخدام غاز الأرجون كغاز حماية طوال العملية.
تم تقييم جودة اللحام من خلال اختبارات الشد والانحناء، و بالفحص الإشعاعي، قياس توزيع الصلادة الدقيقة، والمحاكاة حيث أظهرت النتائج تفوقاً واضحاً في الأداء للأقطاب الهجينة مقارنة بالأقطاب التقليدية، ومن بين جميع الوصلات التي تم اختبارها، حقق القطب الهجين (MX2) عند تيار 70 أمبير أعلى مقاومة شد، حيث بلغت حوالي 772 ميجا باسكال — مع قيم استطالة تجاوزت 100%، وقد أظهر الفحص الإشعاعي لهذه اللحامات وجود عدد قليل جداً من العيوب الداخلية،

بناءً على النتائج التي توصلنا إليها، يبدو أن تيارات اللحام في النطاق من 60 إلى 70 أمبير هي الأنسب لهذه السبيكة وهذا السُمك.

الكلمات المفتاحية: الصلب الذي لا يصدأ AISI 304، لحام TIG، لحام القوس بغاز التنجستين (GTAW)، قطب التنجستين، القطب الهجين، مقاومة الشد، الفحص الإشعاعي، الصلادة، تحليل العناصر المحدودة.

1. Introduction

AISI 304 is among the most commonly used austenitic stainless steels in industry. Its resistance to corrosion, ease of forming, and reliable mechanical behavior make it a practical choice for food-processing lines, pressure vessels, petrochemical piping, and structural components-applications where material failure is not an option. (Davis, 1994)

Gas Tungsten Arc Welding (GTAW), or TIG welding, is the standard process for joining this steel in most fabrication shops. It gives good surface quality and allows the welder to manage heat input carefully—something that matters a lot with 304, which is sensitive to heat-induced microstructural changes. That said, the final weld quality does not depend only on current or shielding gas; the tungsten electrode itself plays a significant role through its effect on arc behavior and heat distribution. (Kou, 2020)

Manufacturers have recently introduced hybrid tungsten formulations claiming improved arc stability and longer electrode life, but there is limited published data comparing these products against established conventional types under controlled conditions. This study was set up to address that gap. We tested nine electrode compositions under identical conditions and evaluated the resulting welds for mechanical performance, internal soundness, and stress distribution using both experimental and numerical methods.

2. Literature Review

The weldability of AISI 304 using TIG processes has been studied extensively, Recent studies have confirmed that welding current and heat input remain among the most influential parameters governing the tensile properties, microstructure, and overall performance of TIG-welded AISI 304 stainless steel joints (Afify et al., 2024; Amalia et al., 2023)

and there is broad agreement that heat input is one of the most influential process variables. Too much heat can promote sigma-phase formation and reduce ductility; too little leads to incomplete fusion or shallow penetration-neither outcome is acceptable in structural fabrication. (Kou, 2020; Lippold & Kotecki, 2005)

Electrode material is another variable that does not receive enough attention in the literature. Pure tungsten works reasonably well in AC applications, but it tends to erode faster under DC conditions. Rare-earth doped electrodes-particularly lanthanotid types—have shown better arc stability and reduced wear in several studies. What is less clear is how the newer hybrid formulations compare to these, especially in terms of weld mechanical properties and radiographic acceptance. (Modenesi et al., 2000)

Recent developments in TIG and hybrid welding technologies have demonstrated that arc stability and heat distribution can significantly influence weld quality, penetration characteristics, and mechanical performance, particularly when advanced electrode systems are employed (Ye et al., 2023)

The present work addresses this by combining tensile testing, radiography, and finite-element modeling in a single, coherent experimental program—an approach that allows direct comparison across electrode types under identical welding conditions.

3. Materials and Experimental Procedure

3.1 Base Material

The base metal was commercially available AISI 304 stainless steel, cut and machined into plates measuring 100 mm × 200 mm × 3 mm. Tables 1 and 2 list its nominal chemical composition and typical mechanical properties.

Table 1. Nominal Chemical Composition of AISI 304 Stainless Steel

Element	Cr	Ni	Mn	Si	C	Fe
wt.%	18–20	8–10.5	≤ 2.0	≤ 1.0	≤ 0.08	Balance

Table 2. Typical Mechanical Properties of AISI 304 Stainless Steel

Property	Value
Yield Strength	≈ 215 MPa
Ultimate Tensile Strength (UTS)	≈ 505–620 MPa
Elongation	≈ 40–60%

3.2 Welding Procedure

Nine electrode types were included in the test matrix:

- Pure Tungsten: WP
- Conventional/Alloyed: WL10, WL15, WL20, WZ8, WS2
- Hybrid: MX1, MX2, MX3

All welds were made with high-purity argon shielding, and three DC current levels were used: 60 A, 70 A, and 80 A. Figures 1 and 2 show the experimental setup and representative welded specimens.

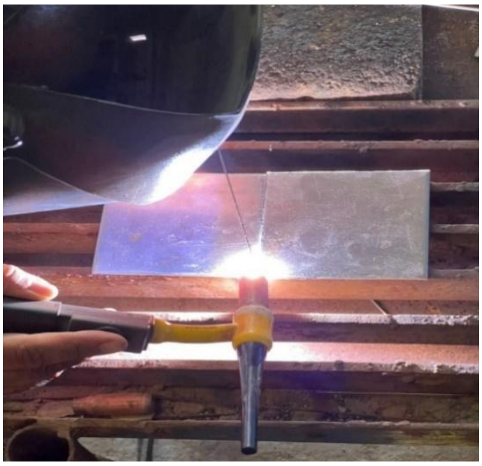

Figure 1. TIG welding operation performed on AISI 304 stainless steel plates.

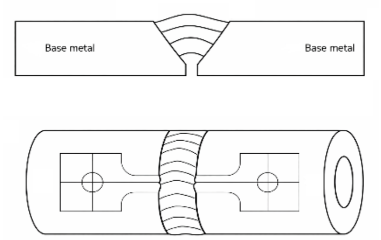

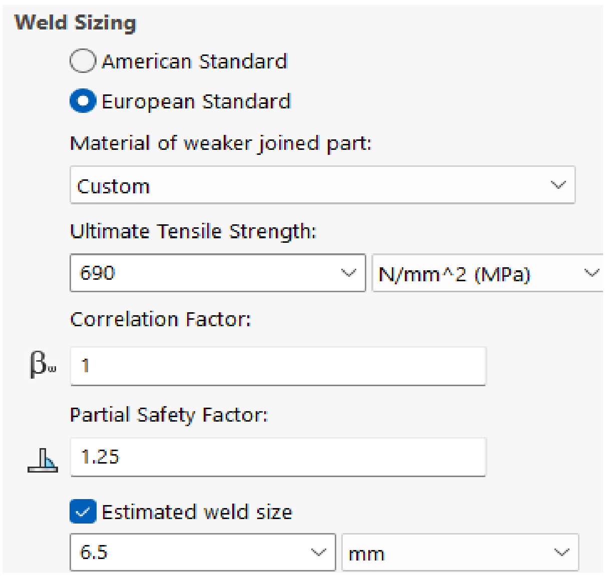

Figure 2. Weld sizing parameters used for numerical modeling showing an estimated weld size of 6.5 mm.

Within the engineering framework, this model is employed to determine the actual tensile stress acting on the weld region, based on the following mathematical formulation: $\sigma = \frac{P}{h*L}$

3.3 Mechanical Testing

Tensile specimens were prepared and tested in accordance with ASTM E8. Bend specimens followed ASTM E290. Figures 3 show the specimen geometry and the testing machine used. Tensile specimens were prepared and tested in accordance with ASTM E8/E8M-22 (ASTM, 2022). Bend specimens followed ASTM E290-22 (ASTM, 2022).

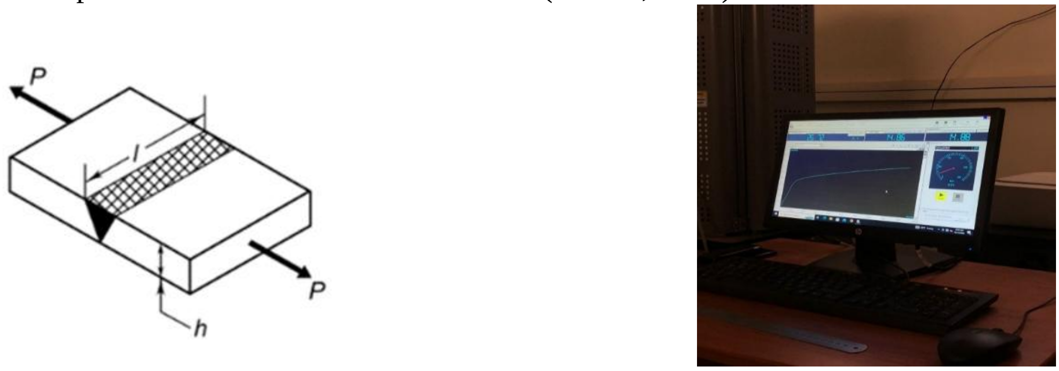

Figure 3. Computerized tensile-testing system used for acquisition of tensile-test data.

3.4 Hardness Testing

Rockwell hardness measurements were obtained from selected welded specimens.

Table 2. Available Hardness Measurements

Specimen	Hardness (HRC)
A	36
B	34

Figure 4. Hardness measurement showing 34 & 36HRC.

3.5 Radiographic Examination

All specimens were radiographically examined to check for subsurface discontinuities, following ASME Section V acceptance criteria. Equipment and sample radiographs are shown in Figures 5 . following ASME Section V acceptance criteria (ASME, 2023).

Figure 5. Representative radiographic image of TIG-welded specimens showing weld continuity and acceptable internal quality.

4. Numerical Simulation

Finite-element analysis was carried out in SolidWorks Simulation as Figure 6 sgowen data formula , Numerical and Multiphysics modeling techniques have become increasingly important tools for predicting thermal behavior, residual stresses, and deformation in GTAW processes, reducing experimental costs and improving parameter optimization (Yeadon, 2022) . The goal was to map stress and strain distributions across the joint under tensile, bending, and torsional loading—conditions that reflect how these joints might be loaded in service. Figures 7 through 10 show the geometric model, mesh, and boundary conditions applied.

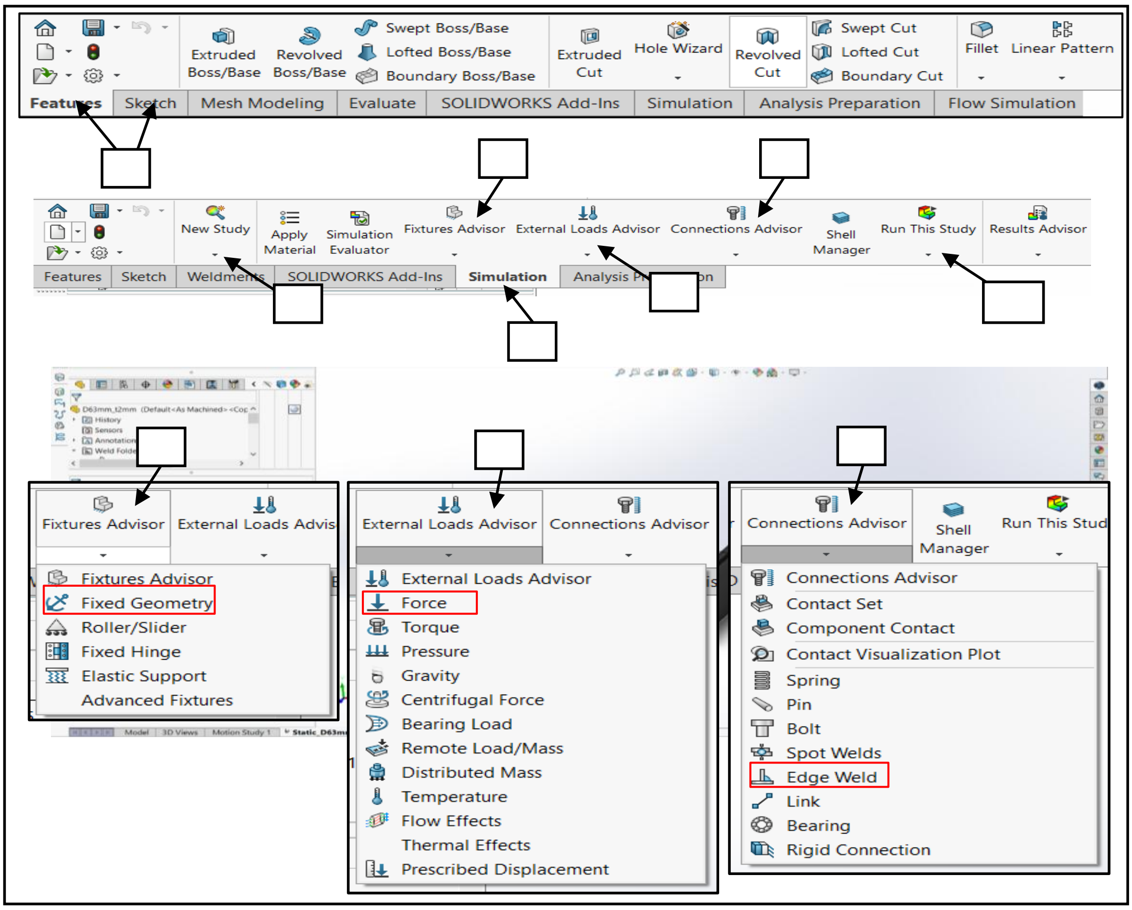

Figure 6. Three-dimensional SolidWorks model of the TIG-welded specimen.

Libyan Open University Journal of Applied Sciences (LOUJAS)
Volume 2 - Issue 2 - 2026 - Pages 62-71

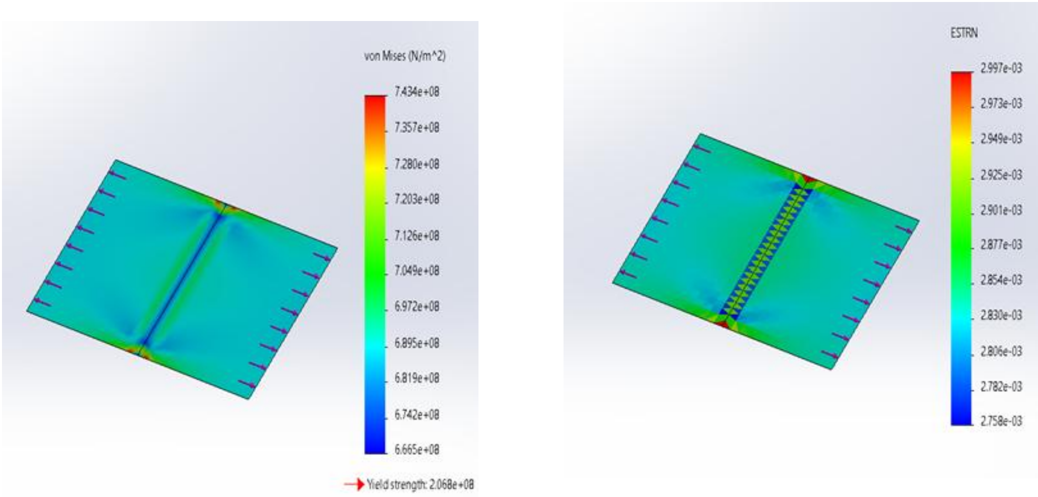

Figure 7. The model was subjected to tensile loading conditions.

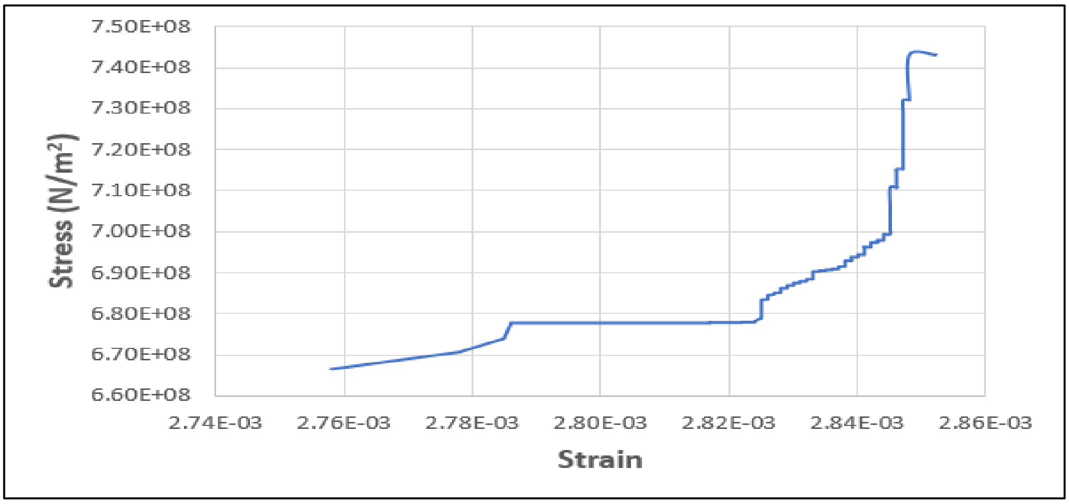

Figure 8. Numerical stress–strain relationship obtained from finite-element simulation.

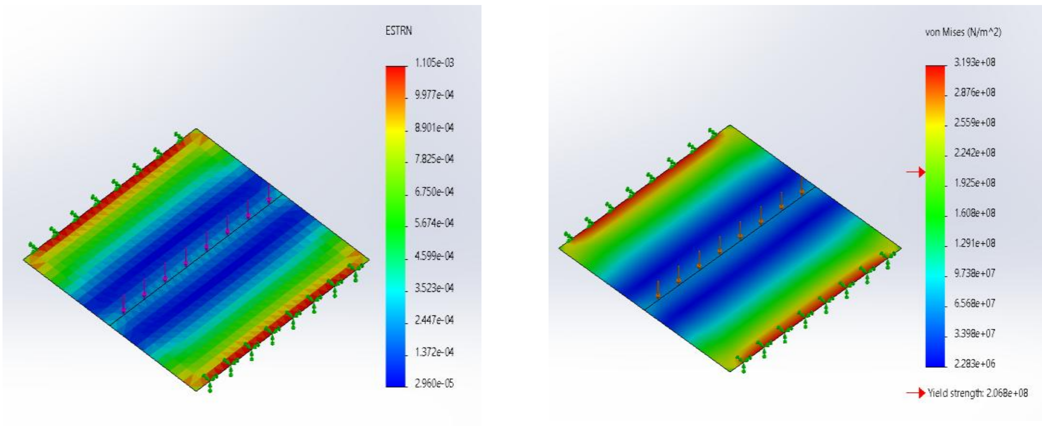

Figure 9 . The model was subjected to bending loading conditions.

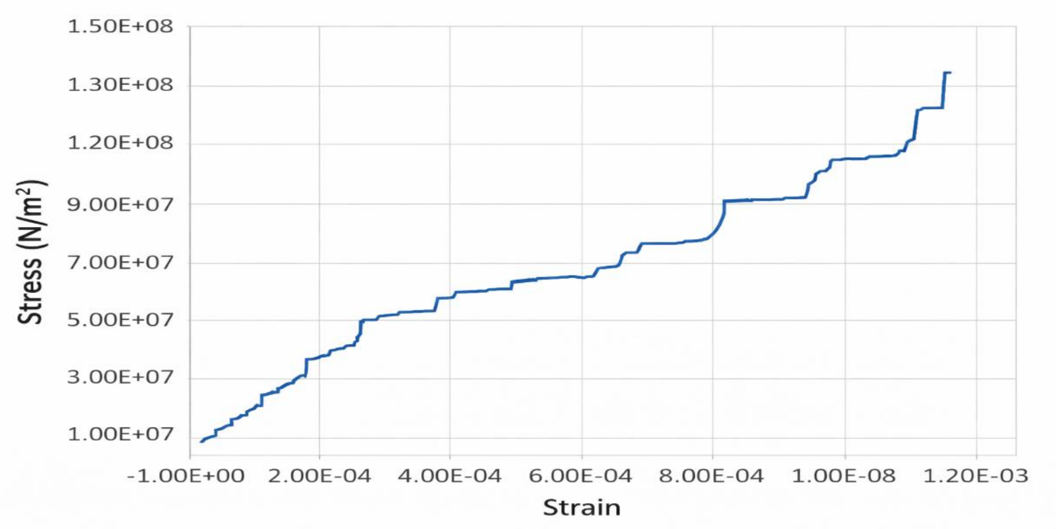

Figure 10. Von Mises stress distribution under bending loading conditions.

5. Results and Discussion

5.1 Tensile Properties

Table 4 summarizes the tensile results. The most immediate observation is that electrode type matters: the pure tungsten WP electrode at 60 A produced the weakest joint (443 MPa UTS), while the hybrid electrodes consistently outperformed all other groups.

Table 4. Experimental Tensile Test Results

Sample	Electrode	Current (A)	Yield Strength (MPa)	UTS (MPa)	Elongation (%)
A	WP	60	213	443	83
B	WL10	70	361	702	110
D	WL20	70	375	733	102
E	WL15	60	406	738	95
F	WS2	80	385	737	95
G	MX1	60	380	730	95
H	**MX2**	**70**	**403**	**772**	**108**
I	MX3	70	401	750	93

Sample H (MX2 at 70 A) reached a UTS of 772 MPa with 108% elongation ,The superior performance observed at intermediate current levels is consistent with previous studies, which reported that optimized welding current improves penetration while minimizing excessive heat input and metallurgical degradation (Afify et al., 2024; Amalia et al., 2023) . The best result in the series. This level of ductility is notably high and likely reflects a combination of stable arc behavior and uniform heat distribution that MX2 appears to provide. The other hybrid electrodes (MX1 and MX3) gave comparable strength values, though with somewhat lower ductility. Figures 11–12 plot UTS, yield strength, and elongation by electrode type.

Table 5. Tensile Properties of Pure Tungsten Specimens

Specimen	ReL (MPa)	ReH (MPa)	Rp0.2 (MPa)	UTS (MPa)
A1	213	214	243	435
A2	212	214	243	450

Customer	Emhemed A1	TestDate	10/12/2025
Coil No/Packet No	A1	Type	Flat
Rm(MPa)	435	ReH(MPa)	214
ReL(MPa)	213	Rp(MPa)	243
Rt(MPa)	267		

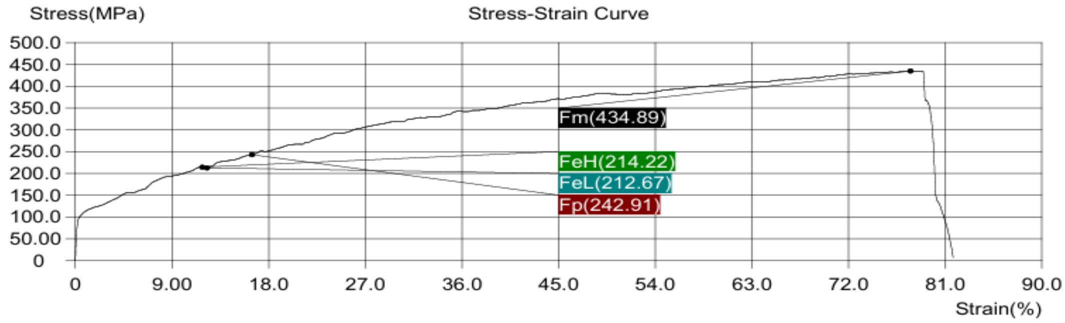

Figure 11. Experimental stress–strain curve of specimen A1 welded using WP pure tungsten electrode.

Customer	Emhemed A2	TestDate	10/12/2025
Coil No/Packet No	A2	Type	Flat
Rm(MPa)	450	ReH(MPa)	214
ReL(MPa)	212	Rp(MPa)	243
Rt(MPa)	275		

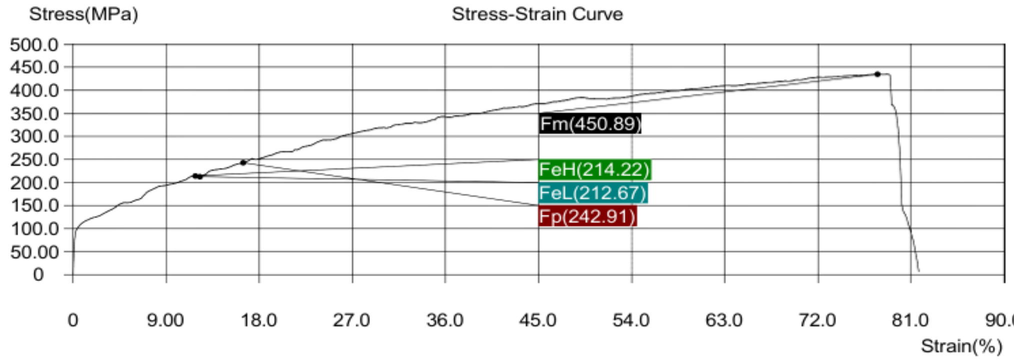

Figure 12. Experimental stress–strain curve of specimen A2 welded using WP pure tungsten electrode.

The stress–strain curves demonstrate substantial plastic deformation before fracture. Despite exhibiting good ductility, the pure tungsten specimens showed significantly lower tensile strength than hybrid-electrode specimens.

5.2 Hardness Results

The measured hardness values ranged between 34 HRC and 36 HRC. The limited variation indicates relatively uniform metallurgical behavior and acceptable thermal control during welding.

5.3 Radiographic Examination

The radiographic results, summarized in Table 6, track closely with the mechanical data. Sample A (the weakest in tension) showed clear evidence of hot cracking—a defect that explains its early failure under load. Samples G and H were free of rejectable discontinuities, though H showed a minor, localized lack of fusion that did not affect its overall performance. Figure (13) shows representative radiographic images from these specimens.

Table 6. Radiographic Evaluation Results

Sample	Observation	Evaluation
A	Hot cracking	Reject
G	Clean weld	Acceptable
H	Minor lack of fusion	Acceptable

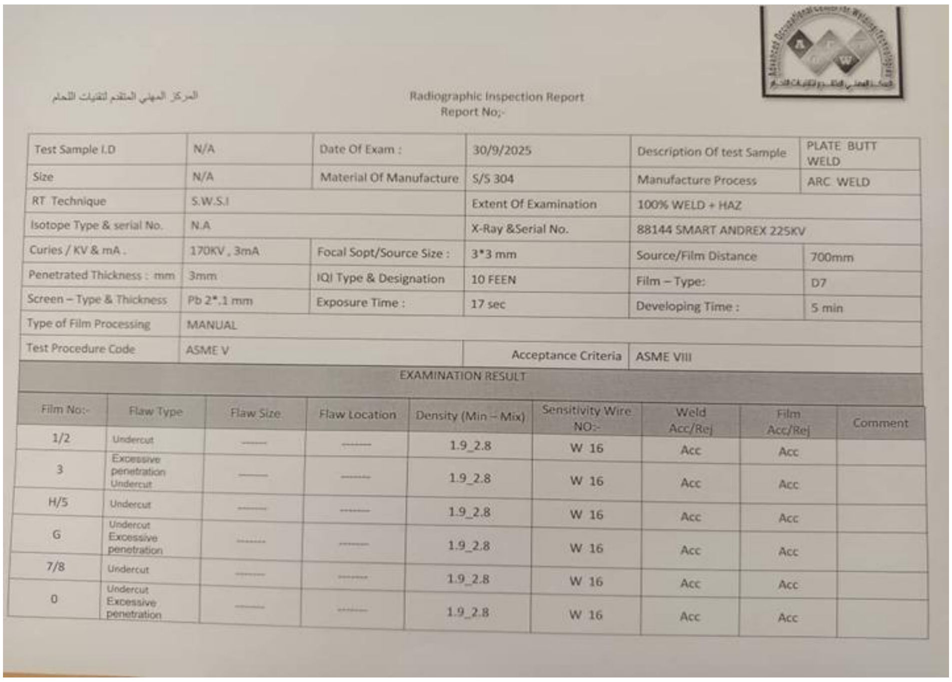

المركز المهني المتقدم لتقنيات اللحام

Radiographic Inspection Report
Report No;-

Test Sample I.D	N/A	Date Of Exam :	30/9/2025	Description Of test Sample	PLATE BUTT WELD
Size	N/A	Material Of Manufacture	S/S 304	Manufacture Process	ARC WELD
RT Technique	S.W.S.I		Extent Of Examination	100% WELD + HAZ	
Isotope Type & serial No.	N.A		X-Ray &Serial No.	88144 SMART ANDREX 225KV	
Curies / KV & mA .	170KV , 3mA	Focal Sopt/Source Size :	3*3 mm	Source/Film Distance	700mm
Penetrated Thickness : mm	3mm	IQI Type & Designation	10 FEEN	Film – Type:	D7
Screen – Type & Thickness	Pb 2*.1 mm	Exposure Time :	17 sec	Developing Time :	5 min
Type of Film Processing	MANUAL				
Test Procedure Code	ASME V		Acceptance Criteria	ASME VIII	

EXAMINATION RESULT

Film No:-	Flaw Type	Flaw Size	Flaw Location	Density (Min – Mix)	Sensitivity Wire NO:-	Weld Acc/Rej	Film Acc/Rej	Comment
1/2	Undercut	------	------	1.9_2.8	W 16	Acc	Acc	
3	Excessive penetration Undercut	------	------	1.9_2.8	W 16	Acc	Acc	
H/5	Undercut	------	------	1.9_2.8	W 16	Acc	Acc	
G	Undercut Excessive penetration	------	------	1.9_2.8	W 16	Acc	Acc	
7/8	Undercut	------	------	1.9_2.8	W 16	Acc	Acc	
0	Undercut Excessive penetration	------	------	1.9_2.8	W 16	Acc	Acc	

Figure 13. shows representative radiographic

5.4 Numerical Simulation Results

The finite-element simulation under tensile loading predicted maximum von Mises stresses approaching 7.43×10^8 N/m² near the weld zone. The corresponding strain distribution indicated localized deformation within the weld region.

The bending simulation predicted a maximum von Mises stress of approximately 3.19×10^8 N/m². Stress concentrations were distributed smoothly across the welded plate, indicating efficient load transfer through the weld.

The numerical stress–strain response demonstrated stable load-carrying behavior and supported the experimental observations.

5.5 Experimental–Numerical Correlation

Comparison between experimental and numerical results revealed good agreement. The simulation successfully identified critical stress locations and reproduced the general behavior of the welded specimens. This agreement supports the validity of the finite-element model and confirms the effectiveness of the selected welding parameters.

6. Conclusions

The following points summarize the main findings from this study:

- Hybrid tungsten electrodes produced stronger, more ductile welds than pure or standard-alloyed electrodes under the same welding conditions.
- The MX2 electrode at 70 A gave the best overall result: UTS of 772 MPa and elongation above 100%.
- Internal defects—particularly the hot cracking seen in the WP sample-were the primary cause of reduced mechanical performance. Radiographic inspection proved useful for identifying these early.

- For 3 mm AISI 304, welding currents between 60 A and 70 A gave the best balance of strength and ductility across electrode types.
- The FE model reproduced the general failure behavior seen experimentally, supporting its use as a screening tool for welding parameter selection.

7. Future work

several aspects of this problem deserve further investigation. Metallographic cross-sections would help explain the microstructural reasons behind the performance differences between electrode types. Residual stress measurements using XRD or neutron diffraction would improve the FE model's accuracy (Lancaster 1999). Fatigue testing under cyclic loading is also needed before these hybrid electrodes can be confidently recommended for dynamic applications. Finally, corrosion testing of the weldments in relevant media would be worth doing, since welding can affect the passive film behavior of 304 in the HAZ."

References

1. American Society of Mechanical Engineers. (2023). ASME boiler and pressure vessel code, section V: Nondestructive examination.
2. American Welding Society. (2020). Structural welding code – Stainless steel (AWS D1.6/D1.6M).
3. ASTM International. (2022). Standard test methods for bend testing of material for ductility (ASTM E290-22).
4. ASTM International. (2022). Standard test methods for tension testing of metallic materials (ASTM E8/E8M-22).
5. Davis, J. R. (Ed.). (1994). Stainless steels. ASM International.
6. Huang, H. Y. (2011). Effects of activated TIG flux on performance of dissimilar welds between mild steel and stainless steel. Journal of Materials Processing Technology, 211, 865–872.
7. Kou, S. (2020). Welding metallurgy (3rd ed.). Wiley.
8. Lancaster, J. F. (1999). The metallurgy of welding. Woodhead Publishing.
9. Lippold, J. C., & Kotecki, D. J. (2005). Welding metallurgy and weldability of stainless steels. Wiley.
10. Modenesi, P. J., Apolinário, E. R., & Pereira, I. M. (2000). TIG welding with single-component fluxes. Journal of Materials Engineering and Performance, 9, 151–155.
11. Afify, R., Abdel-Aleem, H. A., & Gamil, M. (2024). Investigating TIG arc weldments for austenitic stainless steel 304 and 304L: A mechanical and metallurgical analysis. Engineering Research Journal, 53(1), 181–188. https://doi.org/10.21608/erjsh.2023.228930.1205
12. Amalia, I., Sinambela, M. L., Tanjung, R. A., & Awali, J. (2023). Analysis of welding current variation of SMAW and GTAW combination welding with double V groove on SS304 stainless steel. SPECTA Journal of Technology, 7(1). https://doi.org/10.35718/specta.v7i1.663
13. Ye, Y., Yang, B., Yang, Y., Pan, Z., Chen, C., & Zhang, X. (2023). Research on the formation, microstructure, and properties of 304 stainless steel AC-DC hybrid TIG welding. Metals, 13(6), 1127. https://doi.org/10.3390/met13061127
14. Yeadon, W. (2022). Multiphysics modelling of gas tungsten arc welding on ultra-thin-walled titanium tubing [Doctoral dissertation, University of Sheffield]. arXiv.